JOURNAL OF
Optical Communications
and Networking

Optical transport network design beyond 100 Gbaud [Invited]

João Pedro,[1,2,*] Nelson Costa,[1] and Sílvia Pato[3]

[1]Infinera Unipessoal Lda, Rua da Garagem 1, 2790-078 Carnaxide, Portugal
[2]Instituto de Telecomunicações, IST, Universidade de Lisboa, Av. Rovisco Pais 1, 1049-001 Lisboa, Portugal
[3]Instituto de Telecomunicações, DEEC, Universidade de Coimbra, Pólo II, 3030-290 Coimbra, Portugal
*Corresponding author: JPedro@infinera.com

Received 8 August 2019; revised 6 October 2019; accepted 8 October 2019; published 11 November 2019 (Doc. ID 374984)

Optical line interface technology has been the key enabler to reduce the cost per bit transported, thus cost-effectively scaling optical transport networks and mitigating or even avoiding the need to roll out or lease additional optical fibers. However, this technology is reaching fundamental limits, hampering the expectation of significant gains in spectral efficiency in the foreseeable future. State-of-the-art line interfaces already exploit symbol rates that are roughly twice those available with the preceding generations to increase per-channel capacity, and this trend is likely to continue. In the short term, harvesting the benefits of introducing these interfaces mostly depends on the installed reconfigurable optical add/drop multiplexer infrastructure. In the longer term, the impact of further increases in the symbol rate also depends on the evolution of the dominant client data rates and on the channel format selection strategies. Considering a reference transport network and extrapolating how client traffic rates and line interface baud rates will evolve, this work presents a preliminary assessment of the potential benefits and shortcomings of state-of-the-art and future generations of line interfaces.

https://doi.org/10.1364/JOCN.12.00A123

1. INTRODUCTION

Optical networks need to constantly evolve to cope with the ever-increasing request for capacity. One of the key improvements in recent years is the wide adoption of optical line interfaces based on coherent detection in metro, regional, and long-haul optical networks. This improvement enabled a tenfold increase in spectral efficiency (SE), from the 0.2 b/s/Hz of legacy 10 Gb/s intensity-modulated with direct-detection (IM-DD) signals to the 2 b/s/Hz of 100 Gb/s quadrature phase-shift keying (QPSK) signals over the same 50 GHz grid [1]. More recent generations of optical interfaces enabled an additional improvement of both SE and capacity, reaching about 8 b/s/Hz and 600 Gb/s per channel [2,3].

The additional capacity of newer generations of optical interfaces results from advances in optical and electrical components that have higher bandwidth and, therefore, enable an increase in the baud rate, and from the adoption of a wide range of modulation formats that range from M-quadrature amplitude modulation (QAM) to time-domain hybrid QAM (TDHQAM) and probabilistic amplitude/constellation shaping (PAS/PCS). Additionally, the digital signal processing (DSP) block used at the receiver (RX) has also evolved, enabling better mitigation of transmission effects as well as the implementation of more efficient forward error correction (FEC). These improvements enabled a very fine granularity of the capacity of optical channels (OChs), thus allowing (i) an equally fine trade-off of capacity versus transparent reach and (ii) a good match between the capacity that needs to be carried and the OCh generated to carry that data. Moreover, lower cost per bit transported can be obtained by augmenting the capacity per optical line interface via operating at higher symbol rates and/or using higher-order modulation formats.

The wide range of channel formats also leads to an increase of SE, which is further increased by using a flexible grid with a granularity of at least 12.5 GHz [4]. Flexigrid also enables the transmission of superchannels [5], which, by being less impacted by optical filtering at reconfigurable optical add/drop multiplexer (ROADM) nodes, enables increasing the maximum transparent reach and/or capacity of optical networks. However, changing all fixed-grid ROADMs (typically built to work on a 100/50 GHz grid) in deployed networks is expensive, and therefore, only newer optical networks usually benefit from the flexigrid approach.

In the absence of a disruptive technology, the latest improvements in optical line interfaces focus mainly on increasing the baud rate to generate higher capacity OChs and on the improvement of the DSP block to provide a more effective mitigation of transmission effects to improve transparent reach or,

alternatively, enable the use of slightly more aggressive (higher capacity) modulation formats. With respect to the optical fiber infrastructure, one of the approaches with the highest potential to increase capacity consists of the enabling of additional low-loss bands of optical fiber, such as L-band, or even the complete low-loss window of optical fiber (multiband transmission) [6,7]. Other approaches, such as using multicore/mode fibers, are still in the distant future, mainly because they require deploying a completely new optical fiber infrastructure, which is one of the most costly options for a network operator to scale the network [8], and on obtaining more mature components designed for operation in multicore/mode optical networks (e.g., ROADMs and optical amplifiers).

This work overviews optical line interface technology and the impact of deploying upcoming generations of line interfaces. First, it focuses on the state-of-the-art line interfaces (operating at up to 70 Gbaud, using up to 64QAM [3,9]) and considering the different characteristics of the ROADM nodes present in today's optical networks. As originally reported in [10], the analysis highlights that exploiting the full capabilities of these interfaces requires state-of-the-art flexible-grid ROADMs at the network nodes. Second, and extending the scope of [10], this work also aims to gain first-hand insight into the expected impact of deploying the subsequent generations of coherent line interfaces, which are foreseen to be capable of operating at, or even beyond, 100 Gbaud in the near future [11–13]. As part of the latter analysis, the possible evolution of client traffic rates is also modeled with a view to understanding how the combined evolution of client- and line-side technology ultimately impacts the maximum achievable network capacity. The novel investigation provides evidence that, although further savings in the number of interfaces are to be expected with future generations of line interfaces, these devices can also contribute to increased blocking probability and spectrum exhaustion.

The paper is organized as follows. Section 2 gives an overview of the optical line interface technology. Section 3 details the expected network and traffic evolution, highlighting how the client traffic rates and line interface baud rate will likely evolve, and describing possible channel format selection algorithms. The method used to estimate the quality of transmission (QoT), based on the Gaussian noise (GN) approximation for nonlinear fiber transmission effects, is described in Section 4. Section 5 presents simulation results obtained on a reference transport network and discusses the potential of state-of-the-art and future optical line interfaces. Finally, the main conclusions are drawn in Section 6.

2. OPTICAL LINE INTERFACE TECHNOLOGY

Optical line interface technology has made a huge leap since the advent of optical communications. While very simple interfaces, consisting mainly of a continuous wave laser followed by a simple modulator at the transmitter (TX) and a single photodetector at the RX, were sufficient to correctly generate and detect IM-DD signals, still enabling the wavelength division multiplexing (WDM) transmission of a comb of signals [14,15], nowadays much more complex optical line interface technology is used. The additional complexity paved the way to improved coherent detection, which enabled using more complex modulation formats and advanced DSP. Orthogonal frequency division multiplexing (OFDM) and multilevel phase modulations (mQAMs) were regarded as the most promising modulation formats when coherent detection emerged as a commercial solution (∼2010 [16]). However, OFDM has not succeeded in metro, regional, and long-haul networks due to its worse optical performance, mainly due to its high peak-to-average power ratio and its sensitivity to phase noise and frequency offset [17].

One of the key advantages of coherent detection combined with advanced DSP is its flexibility. Due to its simplicity and good optical performance, QPSK was the modulation format of choice for the first generation of coherent optical interfaces. This generation operated at a nominal frequency of ∼10 GHz (40 Gb/s signals) or 25 GHz (100 Gb/s signals) [16]. Further developments in electronics enabled the improvement of the DSP block by using better algorithms for the mitigation of fiber transmission effects, and by using soft-decision (SD) FEC instead of hard-decision (HD) FEC [18,19]. These improvements paved the way to exploiting higher-order modulation formats, mainly 8QAM (150 Gb/s) and 16QAM (200 Gb/s). The most recent developments in both optical and electrical components enabled further improvement of the capacity of line interfaces. Nowadays, modulation formats ranging from QPSK, or even binary phase-shift keying, up to 64QAM and with baud rates up to 70 Gbaud are available, enabling the generation of optical signals with up to 600 Gb/s in a single wavelength [20].

The next generation of optical interfaces will most likely follow the same trend, since no disruptive viable technology has been proposed in recent years. Figure 1 highlights the dimensions exploited by optical interfaces to generate the channel format appropriate for each request. Further advances in optical and electrical components will enable the continuous increase of bandwidth of optical and electrical components, which is expected to lead to interfaces operating at at least 100 Gbaud and with even more complex modulation formats such as TDHQAM or PAS. A summary of the evolution of optical line interfaces is highlighted in Table 1, where it is shown that, depending on the selected modulation format and baud rate, optical signals with a wide range of bit rates may be generated by the same optical line interface. However,

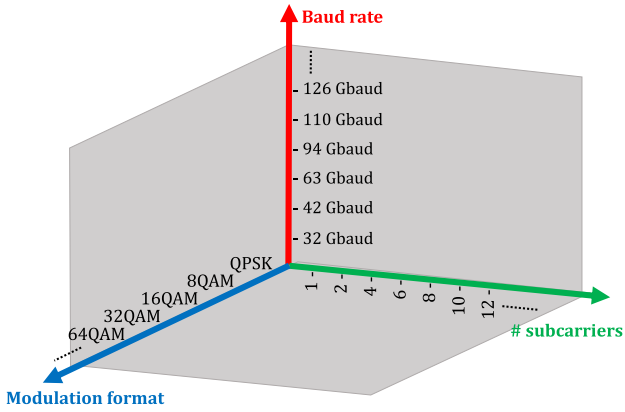

Fig. 1. Main strategies to increase channel capacity.

Table 1. Summary of Optical Line Interface Characteristics

Interface Generation	Approx. Baud Rate [Gbaud]	Grid [GHz]	SE [b/s/Hz]	Modulation Format	Capacity [Gb/s]
IM/DD	10	50	0.2	IM	10
First gen.	12.5/30	50	0.8/2	QPSK	40/100
Second gen.	30	37.5	2–4	QPSK-16QAM	100–200
Third gen.	30–70	37.5–100	2–8	QPSK-64QAM (mQAM)	100–600
Next gen.	30–90	37.5–125	2–8	mQAM/PAS/TDHQAM	100–800

independently of the technology used, there is always a trade-off between reach and capacity as higher-order modulation formats have smaller tolerance of transmission impairments. As an example, 100 Gb/s QPSK is typically the channel format of election for multispan submarine links with total transmission distances on the order of several thousands of kilometers, whereas 600 Gb/s 64QAM is mostly limited to single-span applications [20]. In addition, SE is critical in state-of-the-art optical transport networks (OTNs), motivating the use of flexible grids with tight channel spacing (e.g., 37.5 GHz) [4]. However, careful planning is required in these cases to avoid prohibitive optical filtering penalties [10].

Using very high-capacity optical line interfaces can be a cost-effective solution when high throughputs are required between two end nodes. Grouping the OChs into a single superoptical channel is also possible to further increase reach by reducing the impact of filtering at intermediate ROADMs [5]. However, this approach does not solve the bottleneck limitation of many current optical networks, resulting from the exhaustion of optical fiber bandwidth. Indeed, and as an example, while a 34 Gbaud signal is usually transmitted in a 50 GHz bandwidth, a 69 Gbaud signal might be transmitted in a 100 GHz bandwidth, resulting in approximately the same SE (for the same modulation format). This effect is also highlighted in Table 1, where it is shown that SE has improved by a factor in excess of 10 with the advent of coherent detection, but it has improved marginally since (e.g., improvement from 2 to ~ 8 b/s/Hz but only for very short connections). In fact, the main advantage of increasing the baud rate (when opting for a higher-order modulation format this is not possible due to reach restrictions) is the capital expenditure (CapEx) and operational expenditure (OpEx) savings resulting from having a single interface in the cases where older generations would require using two, or even three, optical line interfaces. Additionally, achieving a very high capacity in a single wavelength may not be the only critical criterion, especially in highly meshed optical networks where communication between many end nodes is required. In these cases, the bandwidth occupied by a single OCh also plays an important role, and reserving just enough bandwidth to transmit the requested data may be critical for an efficient utilization of the optical fiber infrastructure.

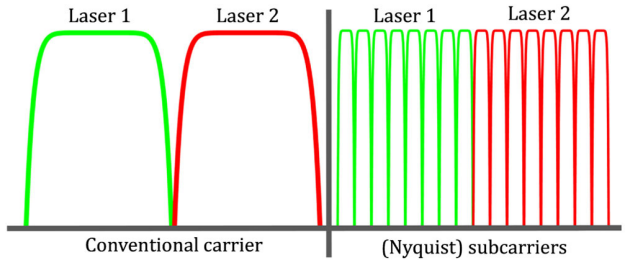

Fig. 2. (Nyquist) subcarriers approach, where a single laser source is used to generate several subcarriers.

A possible approach to improving spectrum usage in highly meshed networks is to transmit several subcarriers in each interface (as illustrated in Fig. 2), which also improves optical performance. As an example, instead of transmitting a single 70 Gbaud signal in 100 GHz, 6×12.5 Gbaud signals can be generated and transmitted within the same bandwidth by a single optical interface, possibly even targeting different end nodes. This approach is more cost-effective as a single optical line interface, which can be potentially implemented using a photonic integrated circuit (PIC), and is able to generate independent lower-capacity carriers to transmit the requested data using the minimum amount of optical fiber bandwidth [3]. Nevertheless, it has the disadvantage of incurring higher filtering penalties, namely, at intermediate ROADMs, when a single laser is used to generate subcarriers that are directed to a larger set of different end nodes.

3. NETWORK AND TRAFFIC EVOLUTION

In order to investigate how network operators can profit from future line interfaces operating at high baud rates, it is necessary to realize some basic assumptions, namely, (i) forecast the evolution of the dominant client traffic rates; (ii) define a set of probable channel formats and their key characteristics (i.e., modulation format, baud rate, carrier count, and frequency slot width); and (iii) describe possible algorithms to select the most suitable channel format to be deployed, depending on the path characteristics and traffic requirements.

A. Ethernet Rates

Transport networks are natively designed to handle a multitude of client signals [21]. Ethernet client signals are increasingly dominant in transport networks, and efforts have been made to better align both technologies. A key historical difference was their rates. In the past, transport network rates increased fourfold, whereas Ethernet rates had a tenfold increase. This was prone to mapping mismatches and, in some cases, resulted in inefficient transport of Ethernet signals over OTNs.

Figure 3 illustrates key milestones in Ethernet rates, as well as two of the upcoming rates, according to the Ethernet Alliance [22]. Particularly relevant to transport networks are the highest rates, which usually target first deployment in core routers. It can be seen that from 100 GbE onwards, each (available) Ethernet rate released is expected to double its predecessor—200 GbE, 400 GbE, 800 GbE, and 1.6 TbE.

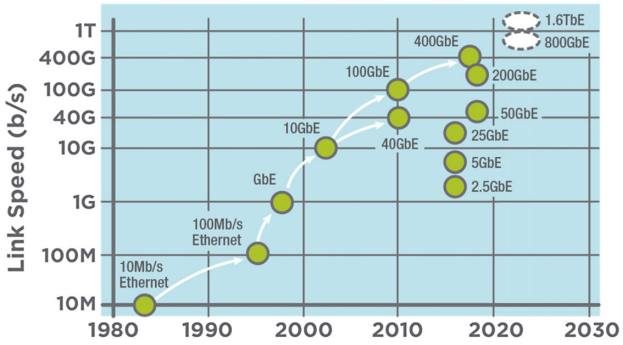

Fig. 3. Ethernet rate evolution (from [18]).

For the purpose of creating traffic matrices associated with Ethernet signals to be carried over a transport network, four different profiles are considered in this work. The first one assumes only 100 GbE signals are to be routed over a transport network and is representative of current deployments. The other three forward-looking future traffic profiles assume two Ethernet rates coexist over the same transport network, with a dominant one accounting for 75% of the traffic, whereas the remaining 25% is assumed to belong to a legacy (lower) Ethernet rate. These specific shares were selected such that there is a clear prevalence of one traffic type (75%), whereas legacy traffic has a smaller, yet still meaningful, share (25%). Table 2 summarizes the four Ethernet traffic profiles used in the case studies reported in Section 5.

B. Optical Channel Formats

The advances in electrical and optical components bound the maximum achievable bandwidth and, consequently, the maximum baud rate made available in each generation of line interfaces. For simplicity, the analysis reported in this work focuses on four main steps in the maximum achievable baud rate, starting with legacy interfaces operating at around 32 Gbaud, followed by state-of-the-art interfaces operating at up to around 70 Gbaud and by two optical line interface generations representative of consecutive steps of additional 30 Gbaud in the maximum baud rate (i.e., up to 100 and up to 130 Gbaud). Albeit state-of-the-art interfaces can be configured to set up OChs with a granularity of 25 Gb/s, in the following, only channel formats capable of a data rate multiple of 100 Gb/s are considered. This decision is supported by the fact that all client signal rates considered are multiples of 100 Gb/s (see Table 2) and have a representative, yet manageable, set of channel formats. Nevertheless, it should be noted that the utilization of Flex Ethernet [23] on both router and transport gear allows matching the client signal size to the capacity provided by the most spectral efficient channel format that can be set up between the end nodes [24].

For an OCh format with N_C optical carriers, modulation format mQAM, a FEC overhead OH_{FEC}, and an extra overhead OH_{nonFEC} (e.g., for OTN framing), the required baud rate to attain a data rate R is assumed to be as given by

$$f_S = \frac{1}{N_C} \cdot \frac{R}{2\log_2 m} \cdot (1 + OH_{\text{FEC}}) \cdot (1 + OH_{\text{nonFEC}}). \quad \textbf{(1)}$$

Table 2. Ethernet Traffic Profiles

Traffic Profile	Ethernet Rate			
	100 GbE	400 GbE	800 GbE	1.6 TbE
100 GbE only	100%	0%	0%	0%
400 GbE dominant	25%	75%	0%	0%
800 GbE dominant	0%	25%	75%	0%
1.6 TbE dominant	0%	0%	25%	75%

In order to avoid unnecessarily enlarging the set of channel formats to be considered, all formats used in this work are assumed to have $OH_{\text{FEC}} = 15\%$ and $OH_{\text{nonFEC}} = 9\%$ [25]. Please note that the same line interface can usually support different FEC types to better match the OCh to the path conditions. However, this dimension is not explored in this work, as the remaining design parameters (i.e., modulation format/baud rate/carrier count/frequency slot) already allow a fine-grained reach/capacity/SE trade-off. The width of the frequency slot allocated to a given channel format, Δf, is given by

$$\Delta f = \left\lceil \frac{N_C \cdot f_S \cdot (1+\alpha) + B}{\Delta f_{\min}} \right\rceil \cdot \Delta f_{\min}, \quad \textbf{(2)}$$

where α denotes the roll-off factor, B is a minimum additional guard band, and $\Delta f_{\min}$ is the frequency grid granularity. A flexible dense WDM (DWDM) grid is assumed. For simplicity, in this work only the following values are used: $\alpha = 15\%$, $B = 2$ GHz, and $\Delta f_{\min} = 12.5$ GHz.

Table 3 characterizes the channel formats supported by different generations of line interfaces according to the above-mentioned assumptions. Only up to two optical carriers are considered per channel format, given that next-generation line cards mostly host two line ports. Note that two channel formats using 64QAM (300 and 400 Gb/s) can be discarded, since they have the same data rate and frequency slot width (i.e., the same SE) while having worse optical performance (reach) than their 32QAM counterparts. As a result, a total of 46 formats is assumed to be made available in the forward-looking line interfaces operating at up to 130 Gbaud. This set reduces to 29 (12) channel formats for line interfaces upper bounded to 100 (70) Gbaud. Finally, only two channel formats are available with legacy 32 Gbaud line interfaces, since this generation of interfaces cannot exploit higher-order modulation formats (i.e., above 16QAM) [10].

From Table 3, it is clear that exploiting higher baud rates enables an increase in the maximum data rate per line interface. Since this is possible for the same modulation format, it translates into having higher capacity with similar transparent reach figures, under the key assumption that implementation penalties are not significantly larger. As a result, savings in CapEx are possible, reducing the cost per bit transported. However, this capacity increase strategy requires allocating spectrum to OChs in approximately the same proportion, resulting in negligible improvements in SE. For instance, considering 16QAM as the reference modulation format, the most spectral efficient options for 70, 100, and 130 Gbaud interfaces all have a SE of around 5.33 b/s/Hz. The main consequence of this is that

Table 3. Channel Format Characterization for Line Interfaces Operating at up to 130 GBaud

Data Rate [Gb/s]	QPSK			8QAM			16QAM			32QAM			64-QAM		
	N_C	f_S [Gbaud]	Δ_f [GHz]	N_C	f_S [Gbaud]	Δ_f [GHz]	N_C	f_S [Gbaud]	Δ_f [GHz]	N_C	f_S [Gbaud]	Δ_f [GHz]	N_C	f_S [Gbaud]	Δ_f [GHz]
100	1	32	50												
200	1	63	75	1	42	62.5	1	32	50						
300	1	94	112.5	1	63	75	1	47	62.5	1	38	50	1	32	50
400	1	126	150	1	84	100	1	63	75	1	51	62.5	1	42	62.5
500				1	105	125	1	79	100	1	63	75	1	53	62.5
600	2	94	225	1	126	150	1	94	112.5	1	76	100	1	63	75
700							1	110	137.5	1	88	112.5	1	74	87.5
800	2	126	300	2	84	200	1	126	150	1	101	125	1	84	100
900										1	113	137.5	1	94	112.5
1000				2	105	250	2	79	187.5	1	126	150	1	105	125
1100													1	115	137.5
1200				2	126	300	2	94	225	2	76	175	1	126	150
1400							2	110	262.5	2	88	212.5	2	74	175
1600							2	126	300	2	101	237.5	2	84	200

available with 32 Gbaud interfaces and subsequent generations
available with 70 Gbaud interfaces and subsequent generations
available with 100 Gbaud interfaces and subsequent generations
available with 130 Gbaud interfaces

when deploying next-generation line interfaces, the expected CapEx savings will not be accompanied by higher overall network capacity. In fact, taking advantage of the higher data rate channels entails a reduction in the number of channels per link, which can result in increased contention for spectrum resources in mesh DWDM networks.

C. Channel Format Selection Algorithms

OTNs are operated over extended periods of time, and traffic demands are set up over these networks along several periods [26]. At each period, a routing, grooming, and spectrum assignment (RGSA) algorithm is used to minimize the CapEx associated with the additional equipment (e.g., line interfaces) that has to be acquired such that all traffic demands and their requirements (e.g., protection) can be satisfied. Both heuristic and integer linear programming (ILP) methods can be used to accomplish this task. A key building block in the optimization process is the decision of which format to deploy, balancing factors such as reach, capacity (provisioned and effectively used), spectral occupation, and SE. Importantly, the format selected when creating a new OCh can target (i) the current (known) traffic needs or (ii) current and future (unknown) traffic requirements. As channels with a wider range of baud rates become available, more options exist and the criteria used can have a larger impact on the overall CapEx and network capacity.

For simplicity, assume that traffic demands are ordered according to a given criterion (e.g., longest distance first) and routed sequentially within each planning period. Note that this is usually the case when a heuristic RGSA is employed during planning or when demands are provisioned via a software-defined networking controller [27]. In the following, it is assumed that demands are aggregated end-to-end (i.e., without intermediate grooming) into OChs. The RGSA algorithm first tries to accommodate the demand into an existing OCh with available capacity. If none exists, a new OCh is created. If no resources are available for this purpose, the demand is blocked.

In this work, two channel format selection algorithms are considered whenever a new OCh has to be created. Let C denote the set of channel formats supported in the network. For a given demand d and a candidate routing path $\pi \in \Pi$, where Π is the set of candidate paths between the demand's end nodes, let $C(d, \pi)$ denote the subset of these formats with enough capacity to carry the demand d that, in the current state of the network, can bridge path π with a minimum number of intermediate reamplification, reshaping, and retiming regeneration points (with respect to all formats in C) and for which there are enough continuous and contiguous spectrum slots. Moreover, let $R(c)$ and $\Delta f(c)$ denote the data rate and frequency slot width of channel format $c \in C(d, \pi)$, respectively. In addition, let $r(d)$ denote the traffic rate of demand d and let $\bar{r}(\pi)$ denote the sum of the data rate of all demands between the same pair of nodes that have not been routed yet in the current planning period. The first algorithm gives priority to selecting the channel format (and routing path) which maximizes SE, breaking ties with the one having the largest capacity. By giving preference to creating a high-capacity channel, future demands between the same node pair may be routed over it, postponing the need to set up another OCh. On the other hand, the second algorithm primarily selects the channel format with a capacity closer to that needed to support all demands between the same node pair, breaking ties by selecting the channel format with minimum spectrum occupation. Therefore, this algorithm minimizes the overprovisioning of capacity and spectrum in the current planning period, but

Most Spectral Efficient with Maximum Capacity (MSE-MaxC)

Input:	Demand d; list of candidate paths, Π; feasible channel formats, $C(\pi)$.
1.	Select channel format(s) $c \in C(\pi)$, $\pi \in \Pi$, with highest SE, i.e., $\max\{R(c)/\Delta f(c)\}$.
2.	Break ties by selecting the channel format with maximum capacity, i.e., $\max\{R(c)\}$.
Output:	Routing path, π^*, and channel format, c^*, selected for deployment.

Just Enough Capacity (JEC)

Input:	Demand d; list of candidate paths, Π; feasible channel formats, $C(\pi)$.
1.	Select channel format(s) $c \in C(\pi)$, $\pi \in \Pi$, with best capacity fit, i.e., $\min\{R(c) : R(c) \geq r(d) + \bar{r}(\pi)\}$.
2.	Break ties by selecting channel format(s) with minimum spectrum occupation, i.e., $\min\{\Delta f(c)\}$.
3.	Break ties by selecting the channel format with highest SE, i.e., $\max\{R(c)/\Delta f(c)\}$.
Output:	Routing path, π^*, and channel format, c^*, selected for deployment.

at the expense of eventually not supporting future demands between these nodes over the OCh created (i.e., requiring the setup of additional channels).

A relevant observation from the channel formats presented in Table 3 is that the support of higher Ethernet rates (Table 2) will require the allocation of larger chunks of spectrum per demand, reducing the number of channels per link. This can result in higher blocking probability, reducing the maximum network capacity. In order to quantify this effect, an alternative considered in the case study investigating the impact of next-generation line interfaces (Section 5) is to exploit inverse multiplexing of client signals, wherein the client demand is split into multiple flows at the source node (e.g., of 100 Gb/s), which are routed independently and merged to recover the client demand at the destination node. The demand is only satisfied if all of the flows can be routed successfully. Importantly, the individual flows being routed via different paths can reach the destination node with diverse delays, which can have a detrimental impact in the protocols running at upper layers, an example being Transmission Control Protocol (TCP) performance degradation. It is possible to mitigate this impact if the transport network enforces differential delay compensation, which ensures traffic (e.g., IP packets) is handed over to the upper layers in the correct order at the expense of electronic buffering in the destination node [28].

4. QUALITY OF TRANSMISSION ESTIMATION

Since modern OTNs rely mainly on modulation formats based on coherent detection, only these are considered in this work. In this case, the optical fiber infrastructure can be simplified as chromatic dispersion compensation and can be performed in the DSP block only, thus avoiding the deployment of optical dispersion compensation units. The performance evaluation of dispersion uncompensated transmission systems employing coherently detected modulation formats can be performed using the GN approach [29,30], which has proven to be quite accurate [28]. The GN model's main assumption is that nonlinear interference (NLI) caused by the Kerr effect can be modeled as additive GN that is statistically independent of signal and amplified spontaneous emission (ASE) noise. Thus, a generalized signal-to-noise ratio (GSNR) at the RX input can be defined as

$$\mathrm{GSNR} = \frac{P_{\mathrm{Tx}}}{P_{\mathrm{ASE}} + P_{\mathrm{NLI}}}, \tag{3}$$

where P_{Tx} is the optical signal average power level, P_{ASE} is the ASE noise power originating in optical amplifiers, and P_{NLI} is the NLI contribution to noise [29,30]. This approach enables taking into account the impact of both linear and nonlinear fiber transmission effects on the SNR in a very simple manner. Incoherent noise accumulation along the link may also be assumed with reduced impact on accuracy, which corresponds to the incoherent GN (iGN) approach [29]. Thus, the total GSNR of a light path that traverses several optical line amplifiers (OLAs) and ROADMs along its path can be given by

$$\frac{1}{\mathrm{GSNR}_{\mathrm{tot}}} = \frac{1}{\mathrm{OSNR}_{\mathrm{add}}} + \sum_{i=1}^{L} \frac{1}{\mathrm{GSNR}_i} + (L-1)\frac{1}{\mathrm{OSNR}_{\mathrm{psth}}} + \frac{1}{\mathrm{OSNR}_{\mathrm{drop}}}, \tag{4}$$

where $\mathrm{OSNR}_{\mathrm{add}}$, $\mathrm{OSNR}_{\mathrm{psth}}$, and $\mathrm{OSNR}_{\mathrm{drop}}$ are the optical SNRs (OSNRs) at the add, pass-through, and drop ROADMs, respectively, and L is the number of optical fiber spans traversed by the lightpath.

Finally, the QoT can be evaluated by calculating the residual margin (RM), defined as the difference between the available SNR and the required OSNR for a given signal quality in back-to-back (B2B). However, in order to cope with additional transmission effects, an additional system margin is also considered. Therefore, the final RM is given by

$$\mathrm{RM} = \mathrm{GSNR}_{\mathrm{tot}} - \mathrm{OSNR}_{\mathrm{B2B}} - \mathrm{Margin}. \tag{5}$$

The system margin results from several contributions. The impact of aging, power ripple along the transmission bandwidth, and polarization-dependent losses is taken into account by considering a fixed system margin of 1 dB. An additional varying system margin is considered. For forward-looking analysis, where line interfaces exceeding 70 Gbaud are considered, and due to the lack of measured data, a variable contribution that depends on the number of network elements along the OCh is considered:

$$\mathrm{Margin} = 1 + 0.05 \times (N_{\mathrm{OLAs}} + N_{\mathrm{ROADMs}}), \tag{6}$$

where N_{OLAs} and N_{ROADMs} are the number of OLAs. For commercial line interfaces (with a baud rate not exceeding 70 Gbaud), a better estimate of the impact of traversing network components, and, namely, ROADMs, is available. In

Table 4. SBN Optical Fiber Parameters

Fiber type	Attenuation Parameter [dB/km]	Dispersion Parameter [ps/nm/km]	Nonlinear Coefficient [1/W/km]
SSMF	0.21	17	1.3

this case, the impact of traversing the cascade of ROADMs is assessed as an OSNR penalty and estimated based on the results shown in [31], but with the symbol rate scaled to the values considered in this study. This OSNR penalty is added to the fixed 1 dB system margin and taken into account when evaluating the RM.

The power launched into each fiber span is optimized in order to maximize the GSNR (LOGO approach [32]). A power level of 1 dBm is set at each ROADM input by a pre-amplifier. The optical signal is assumed to be attenuated by 15 dB when adding or dropping the signal and by 18 dB in the express ROADMs. A noise figure (NF) of 6 dB is assumed for erbium-doped fiber amplifiers (EDFAs). An additional loss of 1 dB at the input and output of the optical fibers, as well as an extra attenuation of 0.01 dB/km due to splice losses, is considered in order to achieve a more realistic modeling of the optical fiber plant. The required $OSNR_{B2B}$ values considered are based on the ones available for state-of-the-art optical line interfaces and are scaled linearly for higher baud rates (i.e., for 100 and 130 Gbaud).

5. RESULTS AND DISCUSSION

A reference transport network is used in this section to realize two case studies. The first one assesses the potential benefits of deploying state-of-the-art line interfaces in existing optical networks, particularly taking into account the impact of the ROADM infrastructure (e.g., DWDM grid and filter cards). The second case study goes one step beyond and aims at understanding how the forecasted evolution of client bit rates and optical line interfaces, as well as the adopted channel format selection algorithm, can impact the network cost-effectiveness and maximum capacity. Therefore, both analyses represent a preliminary assessment of the potential benefits and shortcomings of current and future generations of line interfaces.

A. Simulation Setup

The Spanish backbone network (SBN) reference topology defined by Telefónica in the scope of the FP7 IDEALIST project, illustrated in Fig. 4 and detailed in [33], is used in both case studies. It covers Spain with 30 ROADM nodes and 56 bidirectional links. The average fiber span length, consisting of standard single-mode fiber (SSMF), modeled as shown in Table 4, is approximately 68 km. The tributary cards hosting the ROADM add/drop ports where line interfaces are connected are based on simple splitter/combiners. In the particular case of this work, each tributary card has 24 add/drop ports. Each network link is assumed to have 4.8 THz of spectrum in the C-band.

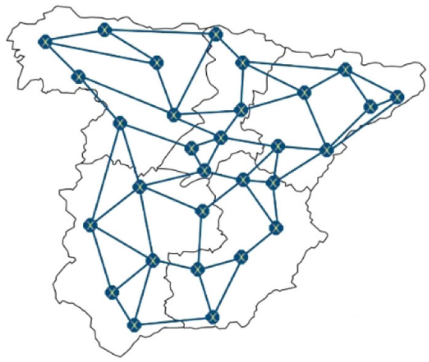

Fig. 4. Spanish backbone network ROADM topology.

B. Impact of State-of-the-Art Optical Line Interfaces

The first case study aims to gain insight into the benefits of deploying state-of-the-art line interfaces (i.e., baud rate < 70 Gbaud) over the SBN, taking into account different ROADM infrastructures. Particularly, two types of ROADM architectures are considered: the broadcast-and-select with colorless add/drop (B&S-C) and the route-and-select with colorless/directionless add/drop (R&S-CD) [34]. As shown in Fig. 5, the former architecture is simpler and resorts to only one wavelength selective switch (WSS) per fiber degree, whereas the latter makes use of more WSSs, granting more flexibility to accommodate traffic dynamics and optical restoration.

In addition, three scenarios are considered with respect to the frequency grid supported and WSS characteristics: legacy fixed 100 GHz grid and legacy 50 GHz grid, both combined with filters/WSSs originally intended to cost-effectively support optical signals with low symbol rates (i.e., < 32 Gbaud), and flexible grid with state-of-the-art WSSs. For legacy fixed 100 GHz and 50 GHz grid, WSSs are modeled as fourth-order Gaussian optical filters with a -3 dB bandwidth of 70 and 40 GHz, respectively [35,36]. For the case of state-of-the-art flexible grid, WSSs are modeled as described in [37], with the bandwidth of the tunable optical filter set to 11.1 GHz and with a -3 dB bandwidth of the WSSs set to 5 GHz smaller than the channel spacing. Figure 6 illustrates the bandwidth reduction resulting from traversing a cascade of WSSs for the three scenarios. Note that for flexible-grid WSSs, the bandwidth reduction as a function of the number of WSSs traversed is shown for three target frequency slot widths (50, 75, and 100 GHz).

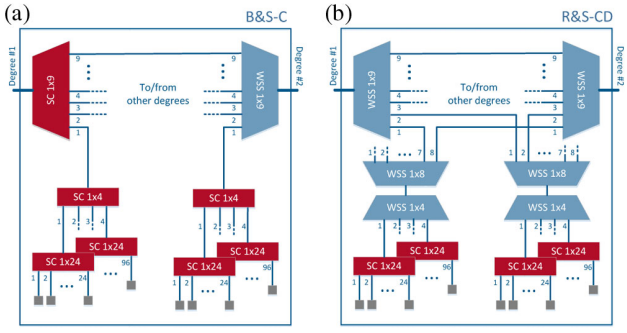

Fig. 5. ROADM architecture for (a) B&S-C and (b) R&S-CD.

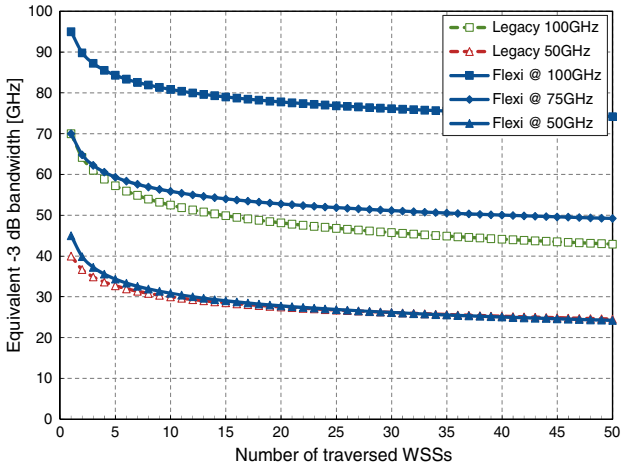

Fig. 6. Bandwidth reduction due to WSS cascade.

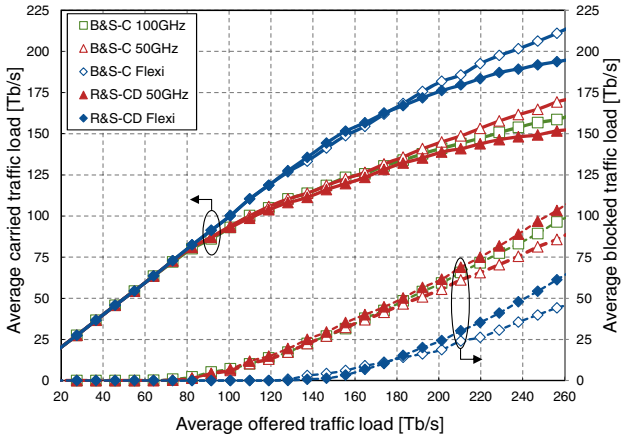

Fig. 7. Network capacity: average carried and blocked traffic load.

Modulation formats include QPSK, 8QAM, 16QAM, 32QAM, and 64QAM. Note that channel formats based on probabilistic amplitude shaping, enabling a slightly better optical performance, or TDHQAM, providing a higher granularity on the trade-off between reach and capacity, could also be considered. However, their usage would not alter the trends observed. The most spectrally efficient format is always used when establishing a new OCh, which corresponds to using the MSE-MaxC algorithm described in Section 3.

Traffic demands are generated in multiples of 100 Gb/s (i.e., the 100 GbE-only traffic profile in Table 2) according to the defined probability distribution function of traffic per node pair [33] and uniformly distributed over 50 consecutive planning periods. At the start of each period, only the traffic demands of that period are known, and an average of 30% of the traffic demands are torn down at the end of each period to enforce traffic dynamics. The traffic demands are first ordered by decreasing the number of links traversed between their end nodes, considering the shortest distance path. For each traffic demand being routed, it is first checked if there is enough idle capacity available in OChs previously provisioned between the same end nodes of the traffic demand. In case there is not enough capacity in these OChs, a new OCh needs to be provisioned. For that purpose, the three shortest routing paths between the end nodes of the traffic demand are considered. Spectrum assignment is performed using the first-fit algorithm. It is assumed that line interfaces are not utilized at intermediate nodes for the sole purpose of wavelength conversion. Note that traffic demands are blocked as a result of a lack of spectrum resources to create new end-to-end OChs using any of the feasible channel formats (restricted to the <70 Gbaud formats in Table 3). Moreover, due to traffic churn, OChs might become empty, in which case the associated line interfaces are released and can be reused, at the nodes where they were originally deployed, to set up new OChs. The results shown are the average over 20 independent simulation runs.

Figure 7 shows the average carried traffic load and the average blocked traffic load as a function of the average offered traffic load when considering the B&S-C architecture with the three grid/WSS configurations and the R&S-CD architecture with legacy 50 GHz and flexible grid. Note that the more advanced R&S-CD ROADM architecture is unlikely to be deployed with legacy 100 GHz filters/WSSs, and, as a result, this configuration is not considered.

The main insight from this set of simulation results is that utilizing state-of-the-art WSSs is paramount in maximizing network capacity. For example, considering the B&S-C architecture, the offered traffic load for a target of 1% blocking probability is ~ 130 Tb/s with flexible grid, whereas it is only ~ 78 Tb/s and ~ 72 Tb/s with legacy 100 and 50 GHz, respectively. This means that roughly 40% less traffic load is supported when resorting to legacy 100/50 GHz. There are different reasons behind this significant reduction in network capacity. First, the utilization of a fixed 50 GHz grid prevents exploiting the enhanced capabilities of state-of-the-art line interfaces, namely, the higher baud rates and the wide array of combinations between baud rate and modulation format. Second, using a fixed 100 GHz grid with WSSs that are not optimized for high symbol rates has a twofold impact, since on one hand it penalizes the performance of the channel formats with higher symbol rates (due to increased filtering penalties), and, on the other hand, it does not allow adaptation of the channel spacing to save spectrum (e.g., when using 32 Gbaud channel formats).

Further evidence of the impact of the above-mentioned limitations can be found in Fig. 8, which shows the average SE of the established OChs (i.e., regardless of their filling ratio) and the average effective SE, which weights the former by the actual capacity being used inside each established OCh. The following observations are due. It can be seen that at low traffic loads, the effective SE is far from the OCh SE, due to overprovisioning of capacity, which is gradually mitigated as the subsequent traffic demands make use of it. Second, it is clear that the use of flexible-grid results in high OCh and effective SE (e.g., with B&S-C up to 5.9 and 5.4 b/s/Hz, respectively), whereas legacy 50 GHz enables a small improvement in SE over the coarser-grained legacy 100 GHz. Finally, these results also highlight that the performance penalty due to the higher number of WSSs used in the R&S-CD architecture can slightly reduce network capacity when compared to the B&S-C architecture.

In order to evaluate the expected impact in terms of network CapEx, two contributions are considered. The most relevant

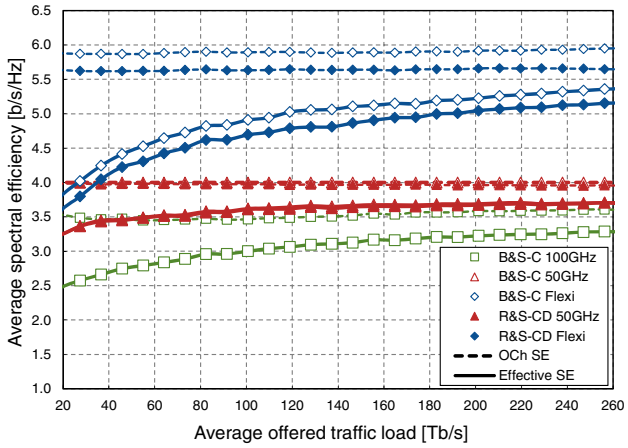

Fig. 8. Spectral efficiency: average optical channel SE and effective SE.

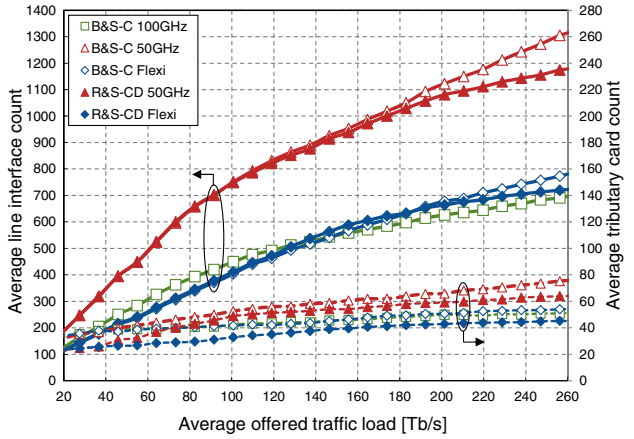

Fig. 9. Network CapEx: line interface and tributary card count.

one is the required number of line interfaces. In addition, the number of tributary cards needed, which depends on the number of line interfaces deployed at each node, is also shown. Figure 9 depicts the evolution of both these quantities as a function of the offered traffic load. It becomes evident that significant savings can be attained when using state-of-the-art (flexible-grid) WSSs or even when using the legacy 100 GHz grid. For instance, for a traffic load of around 73 Tb/s with the B&S-C architecture, the average number of line interfaces required is 306, 363, and 596, for flexible grid, legacy 100 GHz, and legacy 50 GHz, respectively. Hence, around 40% line interface savings are possible when the installed ROADM infrastructure is the legacy 100 GHz instead of the legacy 50 GHz, since the latter prevents the use of channel formats with higher baud rate and higher-order modulation format, which are key to increasing the capacity per channel/line interface pair. Moreover, around 15% additional line interface savings can be attained if the ROADM infrastructure is flexible-grid compliant instead of relying on the legacy 100 GHz. This improvement is due to the fact that flexible-grid WSSs introduce smaller filtering penalties when compared to legacy 100 GHz WSSs, thereby enabling improved optical performance, which in turn allows provisioning some OChs using channel formats with higher capacity.

C. Impact of Next-Generation Optical Line Interfaces

The second case study considers state-of-the-art and next-generation line interfaces. The main goals of this study are to gain insight into the expected line interface savings enabled by the next generation of optical interfaces, as well as on their impact in the maximum achievable network capacity. Note that the number of line interfaces is used as a metric to compare the expected impact in network CapEX for each scenario. A more comprehensive comparison of CapEx figures would require modeling the cost of the different generations of line interfaces, which cannot be reliably achieved in view of the lack of realistic cost figures for hardware that is not commercially available.

Table 5. Line Interface Deployment Scenarios

Traffic Profile	Line Interface Generation			
	32 Gbaud	70 Gbaud	100 Gbaud	130 Gbaud
100 GbE only	√	√		
400 GbE Dominant		√	√	
800 GbE Dominant			√	√
1.6 TbE Dominant				√

Only R&S-CD ROADMs are assumed in the study case. The traffic pattern utilized, given as the probability distribution function of traffic per node pair, is also as defined [33]. The traffic demands are uniformly distributed over 20 consecutive planning periods, and at the start of each period only the traffic demands of that period are known (traffic churn is not present in this case).

The same routing assumptions as described for the previous case study are considered. In addition, network simulations consider both channel format selection algorithms, JEC and MSE-MaxC. In order to include in modeling the evolution of the dominant client signals, Table 5 summarizes the different combinations of traffic profile and line interface generation considered. The results shown are also the average over 20 independent simulation runs.

For the seven combinations of line interface generations and traffic profiles and using the JEC algorithm, Figs. 10 and 11 show the average number of line interfaces and the average carried traffic load as a function of the average offered traffic load, respectively. Regarding the former results, it can be seen that the introduction of each line interface generation, which operates with higher baud rates than the preceding one, enables a reduction in the number of interfaces, which will translate into CapEx savings. This holds, even taking into account the expected evolution to higher Ethernet rates. For instance, for a total average traffic load of around 73 Tb/s, the number of interfaces decreases from nearly 720 with 32 Gbaud interfaces (100 GbE clients) to around 490 when moving to

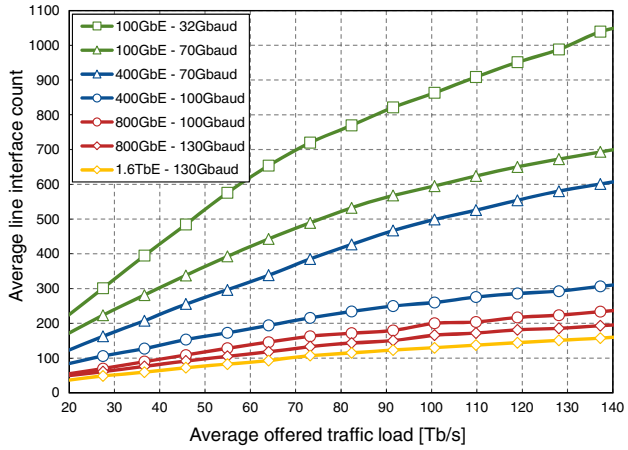

Fig. 10. Average line interface count, JEC algorithm.

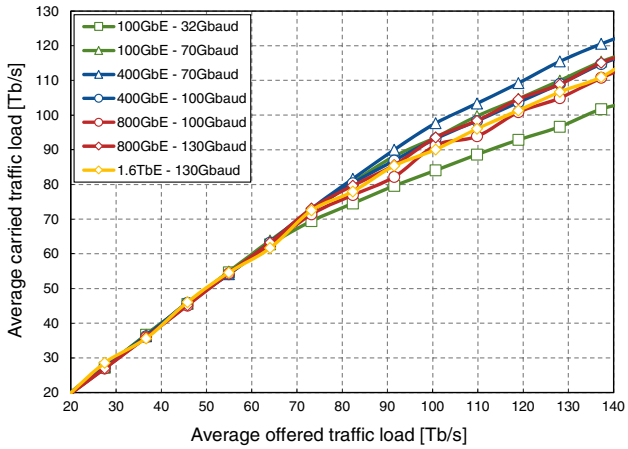

Fig. 11. Average carried traffic load, JEC algorithm.

70 Gbaud interfaces (same client traffic) and to only 107 when adopting 130 Gbaud interfaces (75% 1.6 TbE clients, 25% 800 GbE clients). Besides the direct reduction in number of line interfaces, it is expected that the additional benefits of next-generation interfaces may include a smaller footprint and lower power consumption. However, it can also be observed that these gains are not necessarily accompanied by the ability to carry more traffic load over the same fiber infrastructure. In fact, although there is a clear improvement in the amount of carried traffic load when deploying 70 Gbaud line interfaces instead of the legacy 32 Gbaud ones, the same does not occur when evolving to interfaces with a higher baud rate. Particularly, the average carried traffic load for the 800 GbE and 1.6 TbE traffic profiles is below that supported with the 400 GbE traffic profile. This is mostly a consequence of using wider frequency slots per channel, increasing contention for spectrum between different node pairs.

The performance of both channel selection algorithms, JEC versus MSE-MaxC, is compared in Figs. 12 and 13, considering the average line interface count and the average carried traffic load, respectively. From the plots, it is clear that the utilization of the MSE-MaxC algorithm enables additional savings on the number of line interfaces, particularly when there

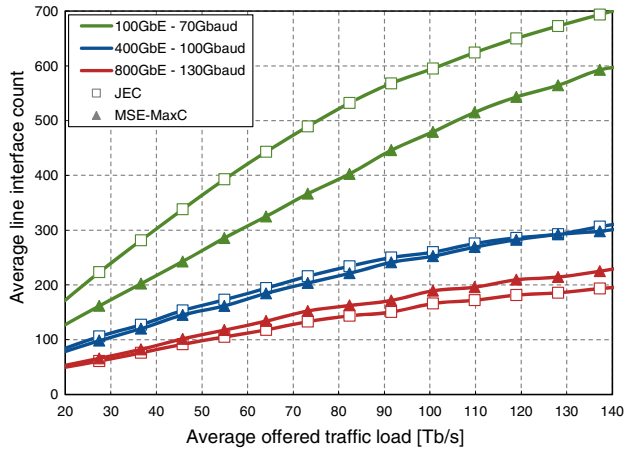

Fig. 12. Average line interface count, JEC versus MSE-MaxC algorithms.

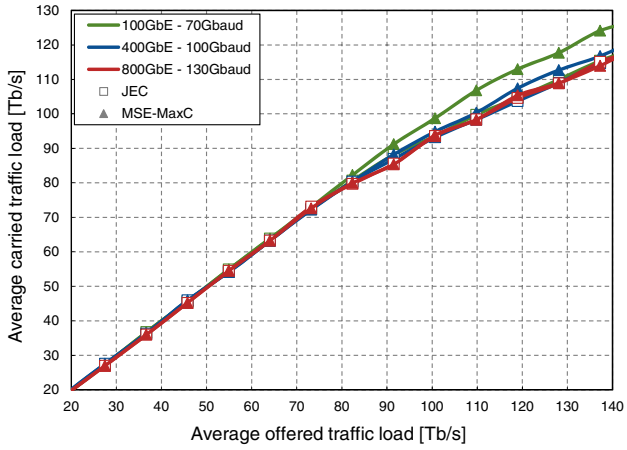

Fig. 13. Average carried traffic load, JEC versus MSE-MaxC algorithms.

is a larger gap between the demand rate and the maximum channel capacity (i.e., the case of 100 GbE with 70 Gbaud interfaces). This is because MSE-MaxC attempts to set up spectrally efficient channels with higher capacity. Even if part of this capacity remains idle in the initial period when the OCh was created, it will tend to be filled as more demands arrive in subsequent periods. Expectedly, as the gap shrinks, the savings reduce, since both algorithms tend to use the same channel formats more often. The simulation results plotted in Fig. 13 also support that the higher SE enabled by the MSE-MaxC algorithm leads to improvements in the carried traffic load, which diminish as line interfaces operating at even baud rates become available for the same reason.

In view of the observed limitation of network capacity when carrying very large Ethernet signals, the last set of results, depicted in Figs. 14 and 15, assesses the impact in the number of line interfaces and carried traffic load of supporting inverse multiplexing of large client signals into 100G flows. Being able to individually route smaller flows allows one to (i) use idle capacity in multiple OChs to carry the same demand and (ii) exploit channel formats with smaller spectrum usage when

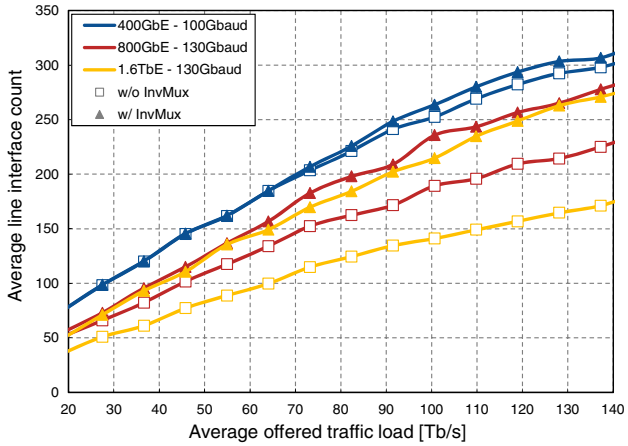

Fig. 14. Average line interface count, MSE-MaxC algorithm with and without inverse multiplexing of client signals.

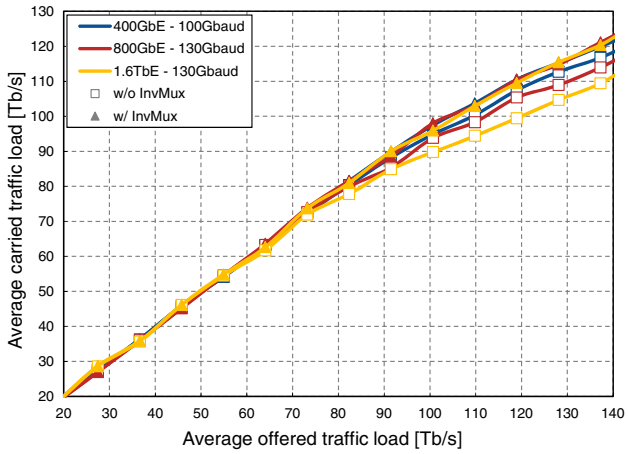

Fig. 15. Average carried traffic load, MSE-MaxC algorithm with and without inverse multiplexing of client signals.

traversing highly congested links. Both effects can potentially reduce demand blocking probability.

An analysis of this last set of simulations results shows that, in fact, the utilization of inverse multiplexing at the end nodes of the traffic demands augments the carried traffic load achieved when routing very large client signals and using line interfaces that exploit high baud rates (Fig. 15). The improvement is particularly evident when supporting client rates of 1.6 TbE. Nonetheless, such improvement is attained at the expense of deploying, in similar proportions, additional line interfaces (Fig. 14). Consequently, it provides evidence that a trade-off is present when having to route large client signals over the transport network; that is, avoiding the penalty in carried traffic load from supporting large client signals requires increasing the number of line interfaces. Note that, since part of the extra line interfaces required are being operated at a reduced line rate, they could be realized using lower baud rate and potentially cheaper interface technology, hence mitigating the foreseen increase in CapEx.

Overall, this preliminary analysis of using future high baud-rate line interfaces to support Ethernet traffic over a mesh transport network highlights that, on one hand, significant savings in line interface count should be expected (eventually coupled with benefits in footprint and power consumption). However, it is clear that the lack of relevant improvements in SE and the added challenge of allocating wider frequency slots in mesh networks to support higher Ethernet rates can hamper the usable capacity of transport networks, providing the motivation to investigate the use of alternative solutions to augment the available spectrum. For instance, in metropolitan and regional networks, using additional spectrum bands besides the C- and L-band may be a viable and cost-effective approach, particularly if rolling out new fiber or leasing additional ones is not possible or is too expensive [38]. Otherwise, it may be unavoidable to resort to multiple parallel fibers, in which case there are reduced possibilities of reducing the cost associated with deploying more fiber, more optical amplifiers, and augmenting the degree of the ROADMs [39].

6. CONCLUSIONS

The potential of state-of-the-art and next-generation optical line interface technology was discussed in this work. Traditionally, the evolution of optical interface technology has been crucial in reducing the cost per bit transported and postponing a possible capacity crunch in optical networks. This paper provided evidence that, while this is still the case when replacing currently deployed interfaces by state-of-the-art ones, especially if the underlying ROADM infrastructure exploits flexible-grid WSSs, in the absence of a technology breakthrough, the next generation of line interfaces will increase the capacity per OCh, mostly at the expense of using more spectrum. As shown in this paper, the consequent reduction in the cost per bit transported will not be followed by an increase in the maximum carried traffic load, and, in fact, it may even reduce this figure when considering future Ethernet rates. Therefore, these conclusions provide a motivation for the need to investigate alternatives to extend the optical fiber infrastructure life cycle, such as multiband transmission, which exploits the low-loss region of optical fibers for data transmission.

Funding. Horizon 2020 Framework Programme (761727); Fundação para a Ciência e a Tecnologia; European Regional Development Fund (UID/EEA/50008/2019).

REFERENCES

1. B. Clouet, J. Pedro, N. Costa, M. Kuschnerov, A. Schex, J. Slovak, D. Rafique, and A. Napoli, "Networking aspects for next-generation elastic optical interfaces," J. Opt. Commun. Netw. **8**, A116–A125 (2016).
2. P. Winzer, "High-spectral-efficiency optical modulation formats," J. Lightwave Technol. **30**, 3824–3835 (2012).
3. https://www.infinera.com/wp-content/uploads/Infinera-Infinite-Capacity-Engine-0025-BR-RevA-0419.pdf.
4. "Spectral grids for WDM applications: DWDM frequency grid," ITU-T Recommendation G.694.1, 2012.
5. J. Pedro, "Designing transparent flexible-grid optical networks for maximum spectral efficiency [Invited]," J. Opt. Commun. Netw. **9**, C35–C44 (2017).
6. A. Napoli, N. Costa, J. K. Fischer, J. Pedro, S. Abrate, N. Calabretta, W. Forysiak, E. Pincemin, J. P. F. Gimenez, C. Matrakidis, G.

Roelkens, and V. Curri, "Towards multiband optical systems," in *Photonic Networks and Devices* (2018), paper NeTu3E.1.
7. A. Napoli, N. Calabretta, J. K. Fischer, N. Costa, S. Abrate, J. Pedro, V. Lopez, V. Curri, D. Zibar, E. Pincemin, S. Grot, G. Roelkens, C. Matrakidis, and W. Forysiak, "Perspectives of multi-band optical communication systems," in *Opto-Electronics and Communications Conference* (2018), pp. 1–2.
8. J. K. Fischer, P. W. Berenguer, B. Shariati, A. Napoli, E. Pincemin, A. Ferrari, V. Curri, N. Costa, and J. Pedro, "Optical multi-band networks: maximizing lifetime of deployed fiber infrastructure," in *Photonic Networks and Devices* (2019), paper NeT3D.3.
9. Y. R. Zhou, K. Smith, S. West, M. Johnston, J. Weatherhead, P. Weir, J. Hammond, A. Lord, J. Chen, W. Pan, C. Cao, R. Yang, N. Zhou, and S. Wu, "Field trial demonstration of real-time optical super-channel transport up to 5.6 Tb/s over 359 km and 2 Tb/s over a live 727 km flexible grid link using 64 GBaud software configurable transponders," in *Optical Fiber Communication Conference* (2016), paper Th5C.1.
10. J. Pedro and N. Costa, "Optical network design towards beyond 100 Gbaud," in *Optical Fiber Communication Conference* (2019), paper M4J.5.
11. J. Zhang, J. Yu, B. Zhu, Z. Jia, F. Li, X. Li, H. Chien, S. Shi, C. Ge, Y. Xia, and Y. Chen, "WDM transmission of twelve 960 Gb/s channels based on 120-GBaud ETDM PDM-16QAM over 1200-km terawave fiber link," in *Optical Fiber Communication Conference* (2016), paper Tu3A.2.
12. J. Yu, J. Zhang, X. Li, and H.-C. Chien, "Generation of 153.6 Gbaud (614.4 Gbps) PDM-QPSK signals and transmission of over 1200 km SMF-28 with EDFA-only," in *Optical Fiber Communication Conference* (2017), paper P2.SC6.19.
13. R. Going, M. Lauermann, R. Maher, H.-S. Tsai, M. Lu, N. Kim, S. Corzine, P. Studenkov, J. Summers, A. Hosseini, J. Zhang, B. Behnia, J. Tang, S. Buggaveeti, T. Vallaitis, J. Osenbach, M. Kuntz, X. Xu, K. Croussore, V. Lal, P. Evans, J. Rahn, T. Butrie, A. Karanicolas, K.-T. Wu, M. Mitchell, M. Ziari, D. Welch, and F. Kish, "Multi-channel InP-based coherent PICs with hybrid integrated SiGe electronics operating up to 100GBd, 32QAM," in *Optical Fiber Communication Conference* (2017), paper Th.PDP.C.2.
14. S. Chandrasekhar and X. Liu, "Impact of channel plan and dispersion map on hybrid DWDM transmission of 42.7-Gb/s DQPSK and 10.7-Gb/s OOK on 50-GHz grid," IEEE Photon. Technol. Lett. **19**, 1801–1803 (2007).
15. M. Wu and W. I. Way, "Fiber nonlinearity limitations in ultra-dense WDM systems," J. Lightwave Technol. **22**, 1483–1498 (2004).
16. https://www.lightwaveonline.com/optical-tech/article/16670750/coreoptics-announces-40g-coherent-msa-transponder-module.
17. J. Armstrong, "OFDM for optical communications," J. Lightwave Technol. **27**, 189–204 (2009).
18. K. Fukuchi, D. Ogasahara, J. Hu, T. Takamichi, T. Koga, M. Sato, E. de Gabory, Y. Hashimoto, T. Yoshihara, W. Maeda, J. Abe, T. Kwok, Y. Huang, K. Hosokawa, Y. Yano, M. Shigihara, Y. Ueki, Y. Saito, Y. Nomiyama, K. Kikuchi, A. Noda, S. Shioiri, M. Arikawa, and T. Wang, "112 Gb/s optical transponder with PM-QPSK and coherent detection employing parallel FPGA-based real-time digital signal processing, FEC and 100 GbE Ethernet interface," in *European Conference and Exhibition on Optical Communication* (2010), paper Tu.5.A.2.
19. G. Tzimpragos, C. Kachris, I. B. Djordjevic, M. Cvijetic, D. Soudris, and I. Tomkos, "A survey on FEC codes for 100 G and beyond optical networks," IEEE Commun. Surv. Tutorials **18**, 209–221 (2014).
20. N. Costa, A. Napoli, T. Rahman, and J. Pedro, "Transponder requirements for 600 Gb/s data center interconnection," in *Signal Processing in Photonic Communications Conference* (2018), paper SpM2G.4.
21. "Interfaces for the optical transport network," ITU-T Recommendation G.709/Y.1331, 2016.
22. Ethernet Alliance, "2019 roadmap," https://ethernetalliance.org/technology/2019-roadmap/.
23. OIF, "Flex Ethernet 2.0 implementation agreement," 2018, https://www.oiforum.com/wp-content/uploads/2019/01/OIF-FLEXE-02.0-1.pdf.
24. A. Eira, A. Pereira, J. Pires, and J. Pedro, "On the efficiency of flexible ethernet client architectures in optical transport networks [Invited]," J. Opt. Commun. Netw. **10**, A133–A143 (2018).
25. G. Khanna, T. Rahman, E. D. Man, E. Riccardi, A. Pagano, A. Piat, S. Calabrò, B. Spinnler, D. Rafique, U. Feiste, H. De Waardt, B. Sommerkorn-Krombholz, N. Hanik, T. Drenski, M. Bohn, and A. Napoli, "Single-carrier 400G 6QAM and 128QAM DWDM field trial transmission over metro legacy links," IEEE Photon. Technol. Lett. **29**, 189–192 (2017).
26. A. Eira, J. Pedro, J. Pires, and J.-P. Palacios, "Optimized client and line hardware for multiperiod traffic in optical networks with sliceable bandwidth-variable transponders [Invited]," J. Opt. Commun. Netw. **7**, B212–B221 (2015).
27. J. Santos, N. Costa, and J. Pedro, "On the impact of deploying optical transport networks using disaggregated line systems," J. Opt. Commun. Netw. **10**, A60–A68 (2018).
28. J. Santos, J. Pedro, P. Monteiro, and J. Pires, "Optimized routing and buffer design for optical transport networks based on virtual concatenation," J. Opt. Commun. Netw. **3**, 725–738 (2011).
29. P. Poggiolini, "The GN model of non-linear propagation in uncompensated coherent optical systems," J. Lightwave Technol. **30**, 3857–3879 (2012).
30. P. Poggiolini, G. Bosco, A. Carena, V. Curri, Y. Jiang, and F. Forghieri, "The GN model of fiber non-linear propagation and its applications," J. Lightwave Technol. **32**, 694–721 (2014).
31. T. Rahman, A. Napoli, D. Rafique, B. Spinnler, M. Kuschnerov, I. Lobato, B. Clouet, M. Bohn, C. Okonkwo, and H. de Waardt, "On the mitigation of optical filtering penalties originating from ROADM cascade," IEEE Photon. Technol. Lett. **26**, 154–157 (2014).
32. P. Poggiolini, G. Bosco, A. Carena, R. Cigliutti, V. Curri, F. Forghieri, R. Pastorella, and S. Piciaccia, "The LOGON strategy for low-complexity control plane implementation in new-generation flexible networks," in *Optical Fiber Communication Conference* (2013), paper OW1H.3.
33. "Elastic optical network architecture: reference scenario, cost and planning," https://cordis.europa.eu/docs/projects/cnect/9/317999/080/deliverables/001-D11ElasticOpticalNetworkArchitecture.doc.
34. J. Pedro and S. Pato, "Impact of add/drop port utilization flexibility in DWDM networks [Invited]," J. Opt. Commun. Netw. **4**, B142–B150 (2012).
35. T. Strasser and J. Wagener, "Wavelength-selective switches for ROADM applications," IEEE J. Sel. Top. Quantum Electron. **16**, 1150–1157 (2010).
36. S. Tibuleac and M. Filer, "Transmission impairments in DWDM networks with reconfigurable optical add-drop multiplexers," J. Lightwave Technol. **28**, 557–568 (2010).
37. C. Pulikkaseril, L. Stewart, M. Roelens, G. Baxter, S. Poole, and S. Frisken, "Spectral modeling of channel band shapes in wavelength selective switches," Opt. Express **19**, 8458–8470 (2011).
38. R. Emmerich, A. Napoli, A. Ferrari, V. Curri, N. Costa, J. Pedro, and J. K. Fischer, "On the prospects of multi-band DWDM transmission," in *Asia Communications and Photonics Conference* (2018), paper S4C.1.
39. J. Pedro and S. Pato, "ROADM express layer design strategies for scalable and cost-effective multi-fibre DWDM networks," in *International Conference on Transparent Optical Networks* (2017), paper Tu.C1.3.